

Technische Universität Berlin
Institut für Hochfrequenztechnik/Photonik
Optische Nachrichtentechnik Praktikum



Laboratory manuskript:

Loss measurement of SOI nano-wires

Created by:

Dipl. Ing. Adrian Juarez
Dr. Ing. Lars Zimmermann

January, 2010

Contents

| | | |
|----------|---|-----------|
| 1 | Introduction | 3 |
| 1.1 | Nanowaveguides | 3 |
| 1.2 | Index contrast | 3 |
| 1.3 | Mode mismatch | 4 |
| 2 | Gratings for coupling in/out light | 6 |
| 2.1 | 1D grating couplers | 7 |
| 2.2 | 2D grating structures | 9 |
| 3 | Waveguide losses | 11 |
| 3.1 | Scattering | 11 |
| 3.2 | Absorption | 11 |
| 3.3 | Radiation | 13 |
| 4 | Experiment | 14 |

1 Introduction

1.1 Nanowaveguides

Silicon photonics based on silicon-on-insulator (SOI) nanophotonic waveguides is a promising technology for integrated photonics due to unique properties of the ultra-high index contrast silicon waveguide systems and due to the use of advanced microelectronics manufacturing technologies. In addition, the use of common process tools and advanced SOI substrates make silicon nanowires a natural choice for integration with advanced microelectronics.

1.2 Index contrast

Nano-waveguides are dielectric waveguides based on the refractive index contrast between a Silicon core and a Silicon oxide cladding as shown in fig.(1.1). Due to the high index of Silicon (≈ 3.5), nano-waveguides differ considerably from more classic waveguide systems such as optical fibers. Optical fibers exhibit a small index contrast between core and cladding, nano-waveguides have a high index contrast. High index contrast results in particular properties of nano-waveguides. Without considering the physics behind these properties, we list in the following the most important features related to the high index contrast.

- increased polarization dependence (birefringence and polarization dependent loss)
- high confinement and small bending loss, leading to the possibility waveguide bends of just a few micron radius
- high intensities in the core of the waveguides, allowing for exploitation of nonlinear properties.

Fig. 1.1 shows the conceptual geometry of the a nano-waveguide in SOI. Solving Maxwells-equations for a symmetrical planar waveguide [4] suggest that the height of the nano-wire needs to be smaller than:

$$h < \frac{\lambda_0/2}{n_1\sqrt{1 - (n_2/n_1)^2}} \quad (1.1)$$

so that single-mode operation is feasible. Assuming for instance $n_1 = 1$, $n_2 = 3.5$ and $\lambda = 1.3\mu\text{m}$ we would obtain a maximal waveguide height of $h = 0.2\mu\text{m}$, which is the height of the nano-wire used in our experiment.

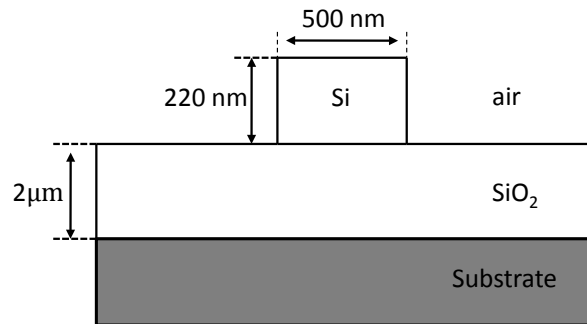


Figure 1.1: Geometry of nano wire used in our Lab

1.3 Mode mismatch

Despite such positive prospects a major stumbling block on the way to nanophotonics applications remains the issue of coupling light in and out of nanophotonic circuits by means of optical fibers. The major problem stems from the large mismatch in modesize of nanowires (\approx a few hundred nanometers) and standard single mode fibers (e.g. SMF28, $\approx 10\mu\text{m}$), which is illustrated in 1.2

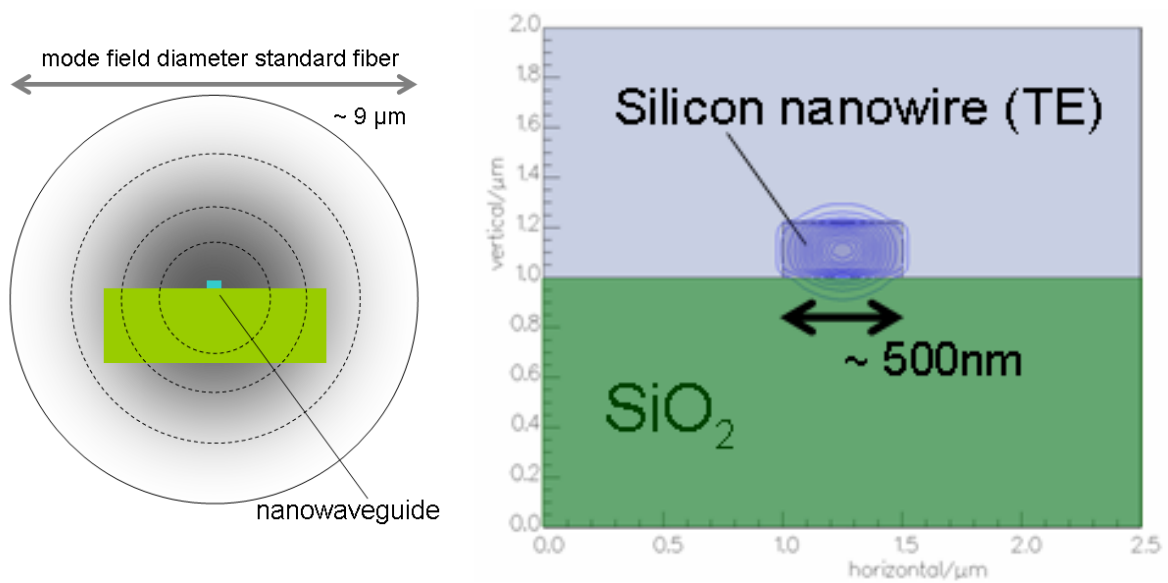


Figure 1.2: Comparison of mode field diameters of standard optical fiber (SMF28) and silicon nanowire waveguide. Nano-waveguide dimensions are typically $\approx 200\text{nm} \times 500 \text{ nm}$.

2 Gratings for coupling in/out light

One solution to this problem is lateral spotsize conversion in an adiabatic taper plus out-of-plane coupling by diffraction via a waveguide grating. The physics underlying the

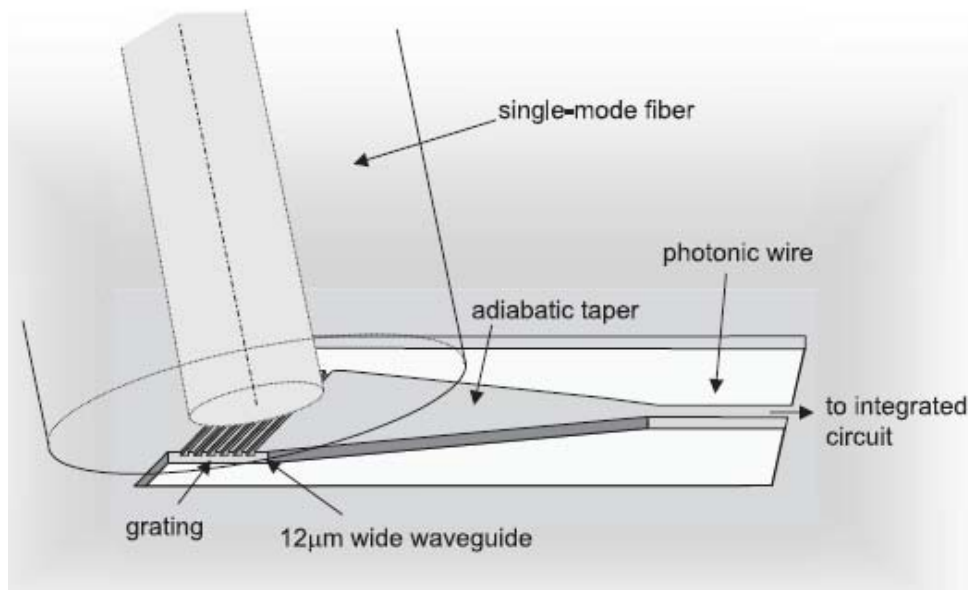


Figure 2.1: Operation principle of a nanowire waveguide grating coupler (Source: D. Tailaert et al., JJAP, 2006)

operation principle of the grating couplers is straight forward. The equation governing this process can be deduced from fig. (2.2). In this simplified arrangement, two rays of light diffract upon a grating surface. If the optical path difference of ray 1 and ray 2 is a multiple of the wavelength λ , constructive interference occurs. Figure (2.2) shows ray 1 undergoing an additional path of \overline{AB} after diffracting, whereas ray 2 undergoes an additional path of \overline{CD} before diffracting. The optical path difference is therefore given by:

$$AB - CD = d(\sin(\Theta_i) + \sin(\Theta_m)) \quad (2.1)$$

If the optical path difference is a multiple of λ , such as:

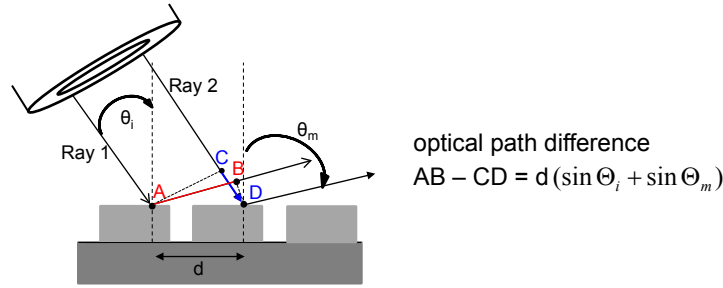


Figure 2.2: Sketch of diffraction principle on a 1D - grating

$$d(\sin(\Theta_i) + \sin(\Theta_m)) = m\lambda \tag{2.2}$$

we have constructive interference. Here m is an integer and is referred as the diffraction order, d refers to the grating period. Grating couplers are usually based on the 2nd order diffraction peak, which couples into the horizontally propagating fundamental mode of the nano-waveguide. The details concerning the grating performance such as efficiency and filter characteristics are tightly connected to the high index contrast and the grating profile. The quantitative characteristics can therefore only be determined by numerical techniques such as FDTD (Finite Difference Time Domain). In the following, we shall just present the basic SOI waveguide grating characteristics without any further reference to grating physics.

2.1 1D grating couplers

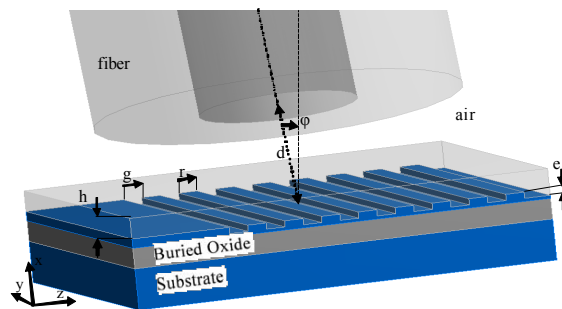


Figure 2.3: 1D grating structure on an SOI nanowire waveguide

The simplest grating coupler is based on a 1D grating structure 2.3. A grating period

consists of a rectangular bar and a rectangular groove. The underlying waveguides are fabricated on 220nm thick SOI. The following features are characteristic for such grating structures:

- high index contrast due to relatively deep etch ($\approx 70\text{nm}$)
- relatively few grating periods (≈ 20)
- tilted coupling out/in (i.e. not under normal incidence)
- only one polarization couples (e.g. TE)

A simulated spectral efficiency distribution is shown in Fig. (2.4). Typical coupling losses between a simple 1D structure and standard fibers are -4 dB. A very important feature

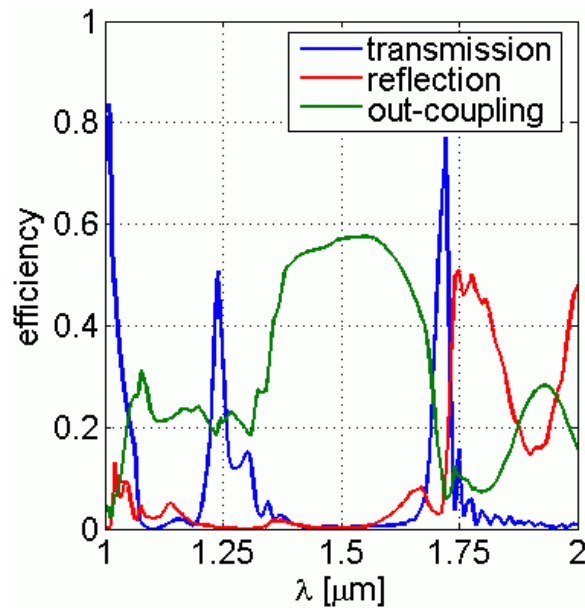


Figure 2.4: Efficiency of a 1D grating structure as a function of wavelength. The grating was optimized for coupling out at 1550nm

of grating couplers is their alignment tolerances with respect to the lateral alignment of the fiber above the grating structure (Fig. (2.5))

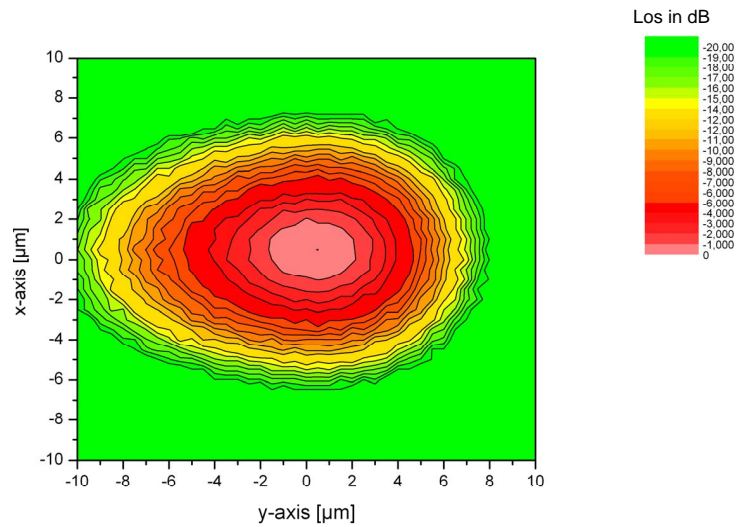


Figure 2.5: Alignment penalty of a standard single-mode fiber when misaligned to a 1D grating coupler. Depicted is the coupling efficiency as a function of displacement.

2.2 2D grating structures

To overcome the polarization dependence of 1D coupling structures the move to 2D grating structures is required. 2D grating structures offer the basic functionality of polarization splitting and rotation. They are therefore useful for polarization diversity schemes. The basic operation principle is depicted in Figure (2.6)

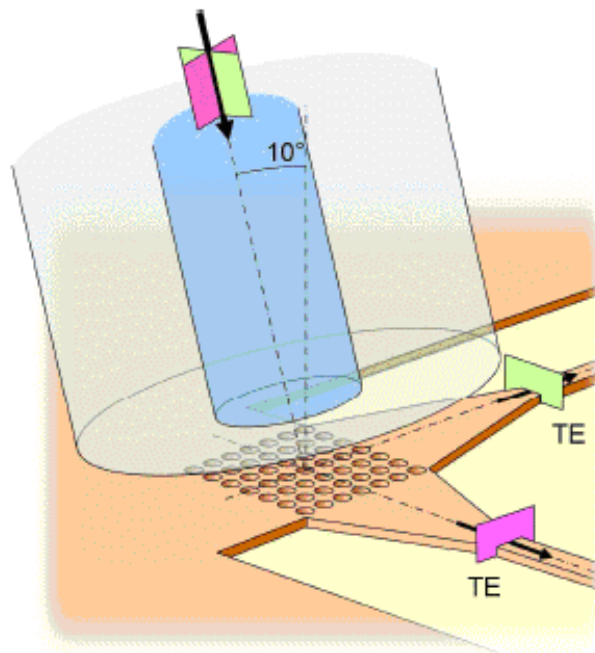


Figure 2.6: A 2D grating coupler decomposes the two orthogonal linear polarizations of the incoming light and couples them to the fundamental TE-modes of the waveguides. This way, polarization diversity can be achieved (Source W. Bogaerts et al, Opt. Express).

3 Waveguide losses

There are mainly three different causes for losses in the optical waveguide: scattering, absorption and radiation [4]. Each of these effects is dependent upon the waveguide design and the quality of the material in which the waveguide is fabricated.

3.1 Scattering

Scattering can appear as volume scattering and interface scattering. The first is found in the bulk waveguide material mainly due to imperfections. These imperfections can appear as voids in the material, contaminant atoms or crystalline defects. Interface scattering is due to the roughness at the interface between the waveguides core and cladding. Usually we can neglect volume scattering and assume only interface scattering. According to [4] the loss coefficient α_s can be approximated by:

$$\alpha_s = \frac{\cos^3 \theta}{2 \sin \theta} \left(\frac{4\pi(\rho_u^2 + \rho_l^2)^{0.5}}{\lambda_0} \right)^2 \left(\frac{1}{h + \frac{1}{k_{y,u}} + \frac{1}{k_{y,l}}} \right) \quad (3.1)$$

where ρ is the r.m.s roughness of the waveguide interface and the index l and u stand for lower interface and upper interface respectively. The parameter k_y stands for the decay constant in y direction and h stands for the waveguide thickness. The propagation angle θ is for each propagation mode different, as well as the decay constants.

3.2 Absorption

Figure 3.1 shows the main reasons for absorption in semiconductor waveguides: band edge (interband) absorption, free carrier absorption and Auger recombinations. Auger recombination plays a minor role and is not described in detail here. Band edge or interband absorption rises for example when photons with energy greater than the band gap

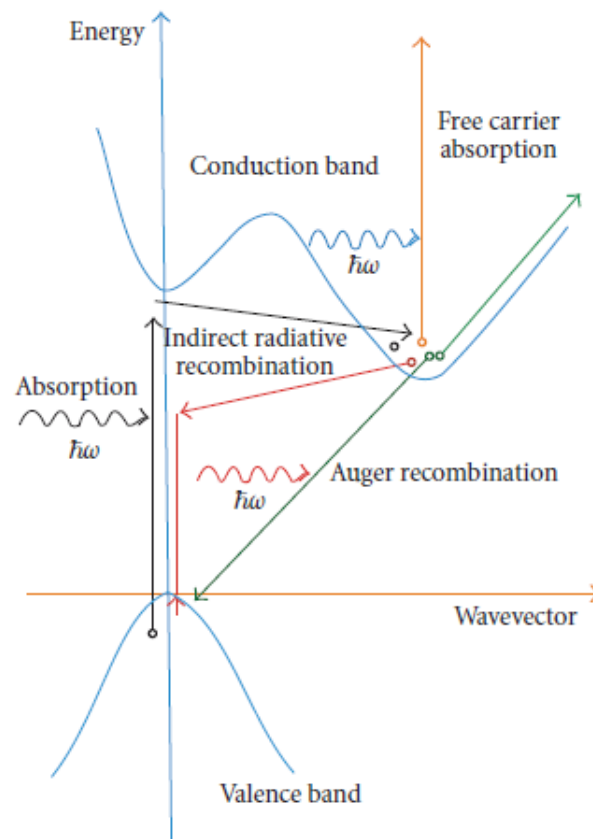


Figure 3.1: Band structure of bulk Si with the various possible transitions for an electron-hole pair: radiative recombination, Auger recombination, and free-carrier absorption.

are absorbed to excite electrons from the valence band into the conducting band. To avoid this kind of absorption it is necessary to use optical wavelengths greater than $1.1\ \mu\text{m}$, which is the band edge of silicon. According to [4] we obtain at a wavelength of $\lambda = 1.52\ \mu\text{m}$ a loss of 0.004dB/cm due to inter band absorption. If one instead decides to use a optical wavelength of $\lambda = 1.15\ \mu\text{m}$ we obtain an absorption loss of $2.83\ \text{dB/cm}$.

Free carrier absorption (intraband absorption) is on the other hand more significant in semiconductor waveguides. Here an electron or a hole absorbs a photon with energy lower than the band gap energy. A Transition from the valence band to the conducting band is not possible for an electron. The transition occurs here within the conduction band. The same idea applies for a hole in the valence band. Changes in absorption can then be described according to [5] by the Drude-Lorenz equation as:

$$\Delta\alpha = \frac{e^3\lambda_0^2}{4\pi^2c^3\epsilon_0n} \left(\frac{N_c}{\mu(m_{ce}^*)^2} + \frac{N_h}{\mu_h(m_{ch}^*)^2} \right) \quad (3.2)$$

where e is the electronic charge; c is the velocity of light in vacuum, μ_e is the electron mobility; μ_{th} is the hole mobility; m_{ce}^* is the effective mass of electrons, m_{ch}^* is the effective mass of holes, N_c is the free electron concentration, N_h is the free hole concentration; ϵ_0 is the permittivity of free space and λ_0 is the wavelength in free space.

3.3 Radiation

This type of loss depends mostly on whether a mode within the waveguide has leakage into the surrounding media; this will mostly be the planar adjacent region to the guide. Mostly, this is not the case and loss due to this effect should be negligible. Radiation can sometimes occur if there are unwanted perturbations in the waveguide exciting higher order modes. The second mode within a single mode waveguide for example is not well guided and in turn suffers leakage. For a multilayer waveguide structure such as the SOI waveguide, the thickness of the buried oxide layer needs to be sufficiently thick so that modes can not couple into the silicon substrate.

4 Experiment

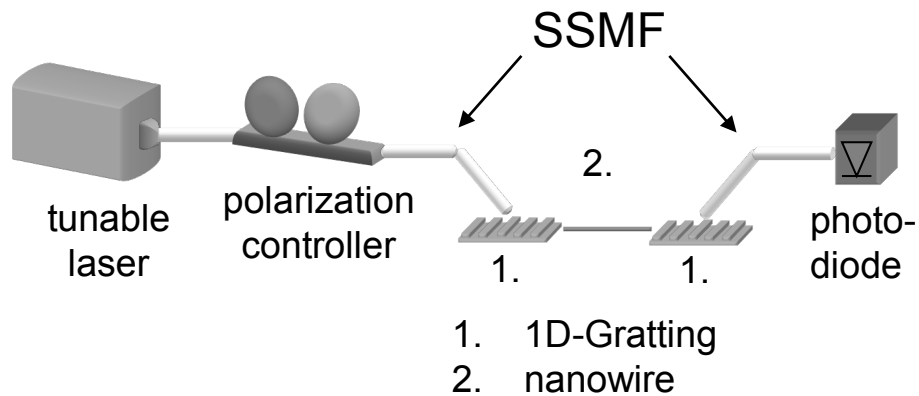


Figure 4.1: Experimental setup

Fig. (4.1) shows the experimental setup. The DFB-laser is centered around the wavelength of $\lambda = 1.55\mu m$. Light couples of the laser into the standard single mode fiber (SSMF) where it propagates into the polarization controller. The latter is used to maximize the coupling efficiency of the 1D grating coupler into the nano-wire. Two fiber holders position the fiber to an angle of about 8 degrees to couple light into the grating coupler no. 1 and out of the grating coupler no.2. After coupling light into coupler no.1 it propagates through the nano-wire, into coupler no.2 where it is redirected into the SSMF. From there the optical wave propagates into the photo diode.

Your task is to measure the average loss in the nano-wire. In order to do so you will use the cut-back method. The principle of the cut-back method is as follows: a waveguide with a certain length L_1 is excited by coupling light into it. The output power P_1 as well as the input power P_0 is recorded. Then the waveguide is shorten or lengthen to a length L_2 while the output power P_2 is recorded. The input power P_0 is kept constant while

doing so. The propagation loss of the length of waveguide ($L_1 - L_2$) is therefore related to the difference in the output power from each measurement [4]. Since we know that the output power is related to the input power as:

$$P_{out} = P_{in} \exp[-\alpha z] \quad (4.1)$$

where z is the propagation length, we can express the output power from both waveguides with length L_1 and L_2 as:

$$\frac{P_1}{P_2} = \exp[-\alpha(L_1 - L_2)]. \quad (4.2)$$

By rearranging Eq. 4.2, we can write α as:

$$\alpha = \frac{1}{L_1 - L_2} \ln(P_2/P_1) \quad (4.3)$$

This equation allows us to calculate the waveguide loss coefficient α as a function of length and power. To increase the accuracy of this technique we can perform various measurements using various waveguide lengths and plotting them. If the coupling losses are the same in all experiments then we have a plot representing the average propagation loss of the waveguide. Fig.4.2 shows a schematic of the various waveguides in the chip. Each color represents N different sets of waveguides with the total length L_i . To fit the total length of the waveguide into the chip the waveguide is folded various times. Here we will assume that the loss associated with the curvature for each turn is negligible.

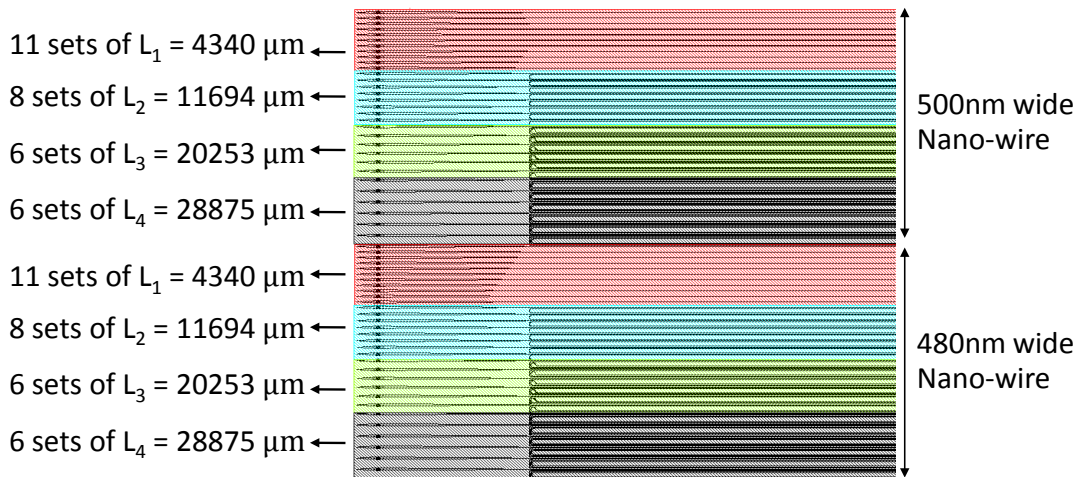


Figure 4.2: Sets of nanowires. Each color stands for a different nano-wire length.

Measurements

- Measure the output power of four nano-wires from each set to determine the average loss of the waveguide with length L_i .
- Determine the loss coefficient α for the nano-wire by interpolating your measurement.
- Calculate with 3.2 the loss due to free carrier absorption. Is this the main cause of loss measured in the nano-wires?

Bibliography

- [1] D. Taillaert, F. Van Laere, M. Ayre, W. Bogaerts, D. Van Thourhout, P. Bienstman, R. Baets, *Grating Couplers for Coupling between Optical Fibers and Nanophotonic Waveguides*, *Japanese Journal of Applied Physics* . (invited), 45(8A), p.6071-6077 (2006).
- [2] W. Bogaerts, D. Taillaert, P. Dumon, D. Van Thourhout, R. Baets, A., *SA polarization-diversity wavelength duplexer circuit in silicon-on-insulator photonic wires*, *Optics Express*, Vol. 15(4), pp. 1567 (2007).
- [3] L. Zimmermann, T. Tekin, H. Schroeder, P. Dumon, W. Bogaerts, *How to bring nanophotonics to application - silicon photonics packaging*, *LEOS Newsletter*, Vol. 22 (6), pp. 4 (2008).
- [4] Graham T. Reed, Andrew P. Knights. *Silicon Photonics, an introduction*, John Wiley and Sons Ltd, England, 2004.
- [5] R.A. Soref, J.P. Lorenzo. *All-Silicon Active and Passive Guided-Wave Components for $h = 1.3\mu\text{m}$ and $1.6\mu\text{m}$* , *IEEE J. Quant. Electronics*, Vol. 22, June 1986.
- [6] R.A. Soref, J. Schmidtchen, K. Petermann. *Large single-mode rib waveguide in GeSi-Si and Si-on-SiO₂*. *J. Quant. Electronics*, Vol. 27, 2003.
- [7] Hecht, Eugene. *Optik, 4 Auflage, 2005*
- [8] Newport, *Diffraction Grating Handbook*,
<http://gratings.newport.com/information/handbook/handbook.asp>